

1 **Application of chemometric modeling for ionic liquid-based ultrasonic-assisted**
2 **dispersive liquid-liquid microextraction: Analysis of fosetyl-aluminum in fruit and**
3 **vegetable samples**

4 Hameed Ul Haq¹, Adil Elik², Hasan Durukan³, Handan Sarac³, Ahmet Demirbas³,
5 Grzegorz Boczkaj¹, Nevcihan Gürsoy⁴ and Nail Altunay^{2,*}

6 ¹*Gdansk University of Technology, Faculty of Civil and Environmental Engineering, Department*
7 *of Sanitary Engineering, 80 – 233 Gdansk, G. Narutowicza St. 11/12, Poland.*

8 ²*Sivas Cumhuriyet University, Faculty of Science, Department of Chemistry, Sivas, Turkey*

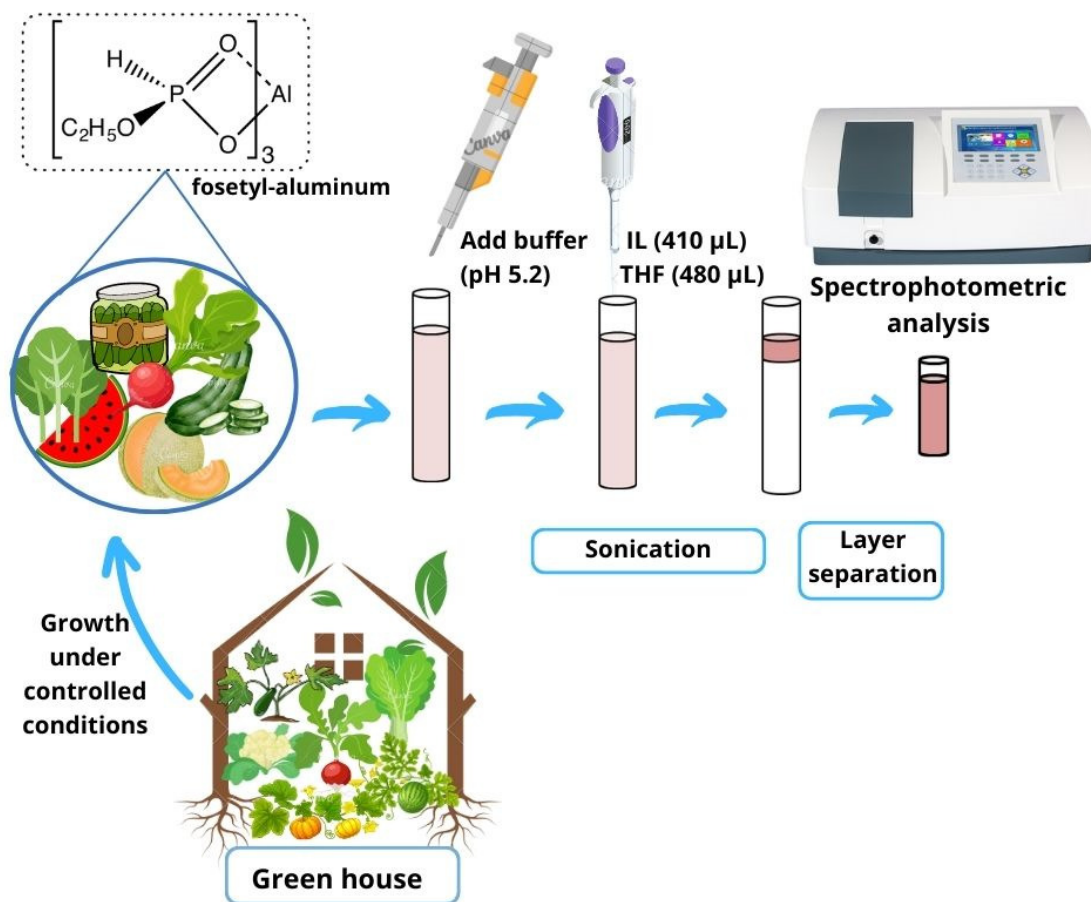
9 ³*Sivas Cumhuriyet University, Department of Plant and Animal Production, Sivas Vocational*
10 *School of Technical Sciences.*

11 ⁴*Sivas Cumhuriyet University, Nanotechnology Engineering, Sivas, Türkiye*

12 *Corresponding author: Email: naltunay@cumhuriyet.edu.tr

13

Graphical abstract



15

16

17

18

19 **Highlights**

- 20 • Ionic liquid-based pre-concentration method for fosetyl-aluminum analysis in foods.
- 21 • Increased mass transfer via DLLME for fungicide isolation from plant material.
- 22 • Fully validated method with proved applicability to real samples and routine analysis.
- 23 • A highly sensitive, selective, and robust assay for environmental monitoring.
- 24 • Fast analyte isolation followed by spectroscopic final determination stage

25

26

27 **Abstract**

28 This manuscript presents a new method for selective extraction and determination of fosetyl-
29 aluminum in fruits and vegetable samples based on ultrasonic-assisted dispersive liquid-liquid
30 microextraction method using ionic liquids (IL-UA-DLLME). A UV-Visible
31 spectrophotometer was used for detection and quantification. Plants used for sample
32 collection were grown under controlled conditions in a greenhouse. Central composite design
33 (CCD)-response surface methodology (RSM) analysis was used for the optimization of
34 significant factors (volume of IL, pH, ultrasonication time, and THF volume). Under optimal
35 conditions, the limit of detection and limit of quantification of the IL-UA-DLLME procedure
36 were 1.5 ng mL^{-1} and 5.0 ng mL^{-1} respectively with relative standard deviation 1.9-3.3%. The
37 developed IL-UA-DLLME procedure demonstrated linearity within the concentration range
38 of $5\text{-}600 \text{ ng mL}^{-1}$ with an R^2 value of 0.9914. The enrichment factor was 114 with a
39 recovery% of 94.2-98.6% (n=3) at optimal conditions. The IL-UA-DLLME assay was used
40 for the analysis of fosetyl-aluminum in a variety of food samples and was found highly
41 selective and efficient.

42 **Keywords:** Food analysis; Food contamination; Organomettalic compounds analysis; Sample
43 preparation; Trace analysis.

44

45

46

47

48

49



50 **1. Introduction**

51 As the population continues to grow at a rapid pace, the issue of nutrition has emerged as
52 a major concern in our era. To enhance the quality and quantity of crops, farmers are widely
53 using pesticides to solve the issues related to presence of undesirable organisms (Tudi et al.,
54 2021). Statistics indicate that herbicides account for 47.5% of all pesticides utilized globally,
55 while insecticides make up 29.5%, fungicides 17.5%, and the remaining 5.5% represent other
56 methods of pest control (Sharma et al., 2019). Fungal plant pathogens are capable of causing
57 significant reductions in crop yield across all agricultural systems globally (Wan de Wouw et
58 al., 2021). The extensive utilization of chemical pesticides has adverse effects on the
59 environment, leading to concerns about pollution. The accumulation of these pesticides on
60 living organisms, pollution of soil and water, and destruction of beneficial organisms are
61 some of the environmental problems caused by their widespread use (Bohinc et al., 2019).
62 Fungal diseases such as mold and mildew can significantly diminish crop yields, making
63 fungicides essential for agriculture and ensuring food safety (Zubrod et al., 2019). To prevent
64 risks related to phytopathogens and increase productivity, fungicides are extensively used
65 (Shahid et al., 2020). Despite their beneficial effects on preventing damage caused by
66 phytopathogens, the detrimental impact of fungicides on soil microbiota's composition and
67 functions is a significant concern for both plant and human health along the food chain
68 (Shahid et al., 2021).

69 Fungicides, which belong to a large group of pesticides, are frequently used in high-yield
70 agriculture to protect plants against the detrimental effects of phytopathogens and enhance
71 crop production. These chemicals are utilized to combat a wide range of fungal diseases and
72 prevent plant infections. It is applied to agricultural production for the preservation of root
73 crops, vegetables, and fruits, or as a direct treatment for ornamental plants, trees, field crops,
74 cereals, and grasses. In a study conducted by Kiselev et al. (2022), it was discovered that



75 fungicides with long-lasting effects, developed for use on potato plants, are capable for
76 effectively suppressing disease development and increasing potato yield. Additionally, these
77 preparations gradually release pesticides into the soil during precipitation or irrigation,
78 reducing the abrupt release of these chemicals. The researchers also noted that these new
79 formulations enable the reduction of pesticide application rates, minimizing the risk of
80 pesticide dispersion and accumulation in the biosphere (Pérez-Lucas, Vela et al. 2019, Tudi,
81 Daniel Ruan et al. 2021).

82 Fosetyl-aluminum is a systemic fungicide that is utilized to manage numerous fungal
83 diseases in plants, such as downy mildew, Phytophthora, and Pythium. It is a phosphonate-
84 derived substance that is usually administered as either a foliar spray or soil drench (Han et
85 al., 2012). Although fosetyl-aluminum has been used for many years, there have been
86 concerns about its potential environmental and health impacts. Some studies have suggested
87 that fosetyl-aluminum may be toxic to aquatic organisms and may accumulate in the human
88 body. There have been also a reports on health effects for humans, such as skin and eye
89 irritation (Han et al., 2012, Rouabhi, 2010). Fosetyl-aluminum is generally considered to have
90 low acute toxicity to mammals, including humans. However, chronic exposure or high levels
91 of exposure may have adverse effects. Studies on laboratory animals have shown that high
92 doses of fosetyl-aluminum can cause reproductive and developmental toxicity, including
93 effects on fertility and fetal development. Additionally, there have been concerns raised about
94 potential carcinogenic effects. Skin contact, inhalation of spray mists, or ingestion of
95 contaminated food or water are potential routes of exposure. Short-term exposure may cause
96 irritation to the skin, eyes, and respiratory system (Authority, Arena et al. 2018, Gormez,
97 Golge et al. 2022).

98 Several analytical methods are available for fosetyl-aluminum analysis including HPLC,
99 flow injection analysis (Sadiq and Hammood, 2022), ion chromatography (Rajski et al.,



100 2018), liquid chromatography-triple quadrupole mass spectrometer (López-Ruiz et al., 2020),
101 liquid chromatography-tandem mass spectrometry (Chamkasem, 2017). However, sample
102 pretreatment/sample preparation is required before analysis. Sample preparation is an
103 important step in analytical methods, where extraction is a commonly used procedure to
104 enhance sensitivity and selectivity. This method involves isolating and concentrating analytes
105 from complex sample matrices like food or biological fluids before analysis (Ullah et al.,
106 2022). Extraction can significantly increase the sensitivity of analytical methods as it reduces
107 matrix effects (Makoś et al., 2018, Haq et al., 2021). Furthermore, extraction can reduce the
108 effects of the sample matrix on the analysis and save time and resources by reducing the
109 volume of the sample matrix (Haq et al., 2023).

110 Ionic liquids (ILs) are a particular type of salts that possess distinctive characteristics such
111 as low volatility, high thermal stability, and adjustable polarity. Due to these characteristics,
112 ILs have been increasingly used as solvents or extractants in various extraction techniques,
113 especially in liquid-liquid extraction. ILs have high solubility for organic and inorganic
114 compounds, making them an effective extractants for a diverse range of samples (Han et al.,
115 2012). Unlike many traditional solvents, ILs are often less toxic, non-volatile, and non-
116 flammable, making them more environmentally friendly. By altering the chemical structure of
117 the cation or anion, ILs can be customized to exhibit high selectivity for particular analytes.
118 This attribute renders them appropriate for extracting analytes from intricate matrices (Llaver
119 et al., 2021). ILs have high thermal stability and do not undergo phase separation or
120 degradation at high temperatures or in the presence of water or other polar solvents
121 (Huddleston et al., 2001). ILs can be easily recovered and reused multiple times, making them
122 a cost-effective and sustainable alternative to traditional solvents (Chiappe et al., 2016). ILs
123 are compatible with many analytical instruments and do not require additional derivatization
124 or extraction steps (Farajzadeh et al., 2020; Rykowska et al., 2018).



125 Central Composite Design (CCD) is an important experimental design technique widely
126 used to optimize analytical methods (Rasheed et al., 2023). It allows for a systematic and
127 efficient exploration of the design space by carefully selecting a limited number of
128 experiments. By incorporating a balanced combination of factorial, axial, and center points,
129 CCD ensures coverage of a broad range of factor settings, facilitating the identification of
130 optimal operating conditions (Chen et al., 2020). CCD is especially useful for detecting and
131 modeling nonlinear relationships between variables. It effectively captures curvature and
132 interaction effects through the inclusion of axial points, resulting in a more precise
133 representation of the response surface. This capability enhances the understanding of complex
134 variable relationships and aids in determining the best combination of factors for optimization
135 (Bahram et al., 2016, Sharma et al., 2022, Chen et al., 2020, Ngan et al., 2014).

136 A novel approach was developed for the extraction and analysis of fosetyl-aluminum in
137 fruit and vegetable samples, utilizing the ultrasonic-assisted dispersive liquid-liquid
138 microextraction technique with an ionic liquid. This method was designed based on the
139 properties and applicability of extraction and is noted for its high sensitivity, selectivity, and
140 versatility over a broad range of concentrations.

141 **2. Materials and methods**

142 **2.1. Instrumentation**

143 A UV-Visible spectrophotometer (Shimadzu 1800 model, Kyoto, Japan) was used for
144 absorbance measurements. A cuvette (Fisher, Germany) made from quartz glass (volume 500
145 μL) was used as sample holder for spectrophotometric measurements. Microwave system
146 (Milestone Ethos, Italy) was used for the digestion of fruit and vegetable samples. Ultra-pure
147 water (18.2 M Ω) was obtained from Milli-Direct Q3 system (Millipore, Bedford, MA, USA).
148 An ultrasonic bath (SK5210LHC Kudos, Shanghai, China) was used for sonication. A pH
149 meter (model 630 Metrohm, Switzerland) with digital pH measuring input for the intelligent



150 pH electrodes from Metrohm, was used for the pH adjustment of samples. The combination
151 electrode consists of two main parts: a pH-sensitive glass membrane and a reference electrode
152 (Ag/AgCl electrode immersed in KCl). A centrifuge (Universal-320 model, Hettich
153 Universal, England) was used to separate the IL phases from the sample solution.

154 **2.2. Chemicals and solutions**

155 The chemicals and reagents used in this research were obtained from Sigma (St. Louis,
156 MO, USA) and Merck (Darmstadt, Germany). All chemicals were of analytical purity and no
157 further purification step was applied. The stock solution (500 mg L^{-1}) of fosetyl-aluminum
158 was prepared by dissolving the appropriate amount of its solid reagent (Merck) in the water.
159 Working and calibration solutions of fosetyl-aluminum were prepared by daily dilution of the
160 stock solution. Tributyl-tetradecylphosphonium chloride (Sigma, $[\text{P}_{4,4,4,14}]\text{Cl}$) ionic liquid
161 was used as the extraction solvent. Tetrahydrofuran (THF) (Merck) was used to disperse IL in
162 the sample solution. Citrate buffer solution (0.1 M pH 5.2) was prepared by dissolving
163 appropriate amount of sodium citrate dihydrate and citric acid in water.

164 **2.3. Sampling**

165 This study was conducted in the greenhouse of Sivas Cumhuriyet University,
166 Department of Crop and Animal Production, using a plastic pots with a capacity of 3 kg. The
167 research followed a randomized plot design, with 3 replications. A soil samples were
168 collected from a depth of 0-20 cm and had a clay loam texture, calcareous (13.8%), salt-free
169 (0.026%), low organic matter content (1.77%), slightly alkaline pH (7.89), low phosphorus
170 content (48.8 kg ha^{-1}) and sufficient potassium content ($1099.5 \text{ kg ha}^{-1}$). In the study, melon,
171 watermelon, collards, gherkin, cauliflower, radish, and zucchini were used as test plants. As
172 basic fertilization, nitrogen 150 mg Kg^{-1} ($\text{CaNO}_3 \cdot 4\text{H}_2\text{O}$), phosphorus 100 mg Kg^{-1} , and
173 potassium 125 mg Kg^{-1} (KH_2PO_4) were applied for all plants with planting. After the plants



174 emerged and reached a certain size, the fungicide containing 80% Fosetyl-Al was added 3
175 times in total, at weekly intervals. 50 days after sowing, the plants were harvested by cutting
176 them from the soil surface. The harvested plants included melons, watermelons, collards,
177 gherkins, cauliflowers, radishes, and zucchinis, which were then left to dry in the shade at
178 room temperature. The dried plants were subsequently grinded using a plant grinding mill,
179 with 1 g of each plant weighed and combined with 10 mL of distilled water (at a ratio of
180 1:10). The mixture was then subjected to maceration, wherein it was shaken for 24 h in a
181 shaker. Following the maceration process, the mixture was filtered with No. 1 Whatman blue
182 band filter paper, and the water was evaporated using a rotary evaporator at 40°C.

183 **2.4. Experimental design**

184 To optimize and design the experimental parameters and perform ANOVA analysis of
185 the analytical data, trial version 11.0.3.0 of the Design-Expert® package from STATISTICA
186 was used. A central composite design-response surface methodology approach was used for
187 the optimization of extraction-affecting factors for fosetyl-aluminum. Four parameters
188 including IL volume (300-900 µL), pH (4-8), ultrasound time (2-10 min), and THF volume
189 (100-500 µL) were optimized using a three-level CCD model. Total 30 experiments
190 (including 6 central experiments) designed by CCD model were performed. Optimized
191 parameters, their units, symbols, and their lowest-highest limits are given in Table S1.

192 **2.5. IL-UA-DLLME procedure**

193 The experimental steps of the IL-UA-DLLME procedure are as follows. First, 10 mL of the
194 digested samples were added to the conical tubes. After this step, the pH of the sample
195 solution was adjusted to pH 5.2 using 0.1 M citrate buffer solution. In order to extract the
196 fosetyl-aluminum in the sample solution, first 410 µL of [P_{4,4,4,14}]Cl (as extraction solvent)
197 and then 480 µL of THF (as the dispersing solvent) were added to the obtained mixture.
198 Conical tubes were placed in an ultrasonic bath and sonicated for 2.5 min at room temperature



199 to effectively disperse the [P_{4,4,4,14}]Cl in the sample solution. At this stage, the [P_{4,4,4,14}]Cl
200 phase containing fosetyl-aluminum was collected on top of the aqueous solution. The
201 [P_{4,4,4,14}]Cl phase was transferred to microcuvettes using a syringe and absorbance
202 measurements were made using UV-spectrophotometer at 289 nm. All these studies were
203 carried out in parallel with the sample blank and standard spiked samples.

204 2.6. Calculations of recovery and validation assay

205 The percent recovery was utilized as a reference in the optimization studies to choose
206 appropriate values for the extraction parameters. The percent recovery was calculated using
207 the following equation 1.

$$208 \quad \text{Percent recovery} = \frac{C_e}{C_a} \times 100 \quad (1)$$

209 In the above equation, C_e is the concentration experimentally determined in the model sample
210 and C_a is the actual/expected concentration.

211 To evaluate the matrix effect of components, the absorbance of the fosetyl-aluminum in the
212 matrix standard and the absorbance of the the fosetyl-aluminum in the solvent standard at the
213 same concentration level were used (Rutkowska et al., 2018).The matrix effect was calculated
214 using the following equation 2.

$$215 \quad \text{Matrix effect} = \left(\frac{\text{absorbance}(\text{matrix standard})}{\text{absorbance}(\text{solvent standard})} - 1 \right) \times 100 \quad (2)$$

216 In analytical chemistry, the relative standard deviation (RSD%) is frequently used to describe
217 the reproducibility of an assay. RSD% for this method was calculated using the following
218 equation 3.

$$219 \quad RSD(\%) = \frac{sy/x}{C_m} \times 100 \quad (3)$$

220 In the above equation, sy/x is the residual standard deviation and C_m is the
221 mean concentration in real samples.

222 In line with the aforementioned method, the enrichment factor (EF) was determined as the
223 ratio between the concentration of the analyte in the final phase, which is prepared for
224 analysis, and that in the initial solution. The EF was calculated using the following equation 4.

$$225 \quad EF = \frac{C_f}{C_i} \quad (4)$$

226 The equation mentioned above uses C_f to represent the final concentration and C_i to represent
227 the initial concentration of fosetyl-aluminum in the acceptor phase (IL phase) and donor
228 phase, respectively. To determine the limit of detection (LOD) and limit of quantification
229 (LOQ), the following formulas (5 and 6) was utilized.

$$230 \quad LOD = \frac{3 \times sy/x}{m} \quad (5)$$

$$231 \quad LOQ = \frac{10 \times sy/x}{m} \quad (6)$$

232 In the above equations, sy/x is the residual standard deviation of regression line and m is the
233 slope of the calibration curve.

234 3. Results and discussion

235 3.1. Optimization of the extraction parameters using a central composite design

236 The CCD is a commonly utilized method for experimental design in the process of
237 optimizing analytical methods. Response surface methodology (RSM) is used to develop a
238 mathematical model that describes the relationship between the response (i.e., the analytical
239 signal) and the independent variables (i.e., the factors affecting the analytical method). The
240 CCD is a common experimental design technique for optimizing analytical methods. The
241 CCD comprises three categories of points: factorial, axial, and center points. Factorial points
242 are ordinary experimental points utilized to ascertain the primary and interaction effects of
243 independent variables. Axial points aid in estimating the curvature of the response surface,
244 while center points are employed to estimate errors in the model. The CCD was used for the
245 optimization of important analytical parameters and statistical analysis of the obtained results.



246 The CCD model was used for the optimization of four analytical parameters, IL volume, pH,
247 ultrasonic time, and THF volume. The parameters were labeled as (A) for IL volume, (B) for
248 pH, (C) for ultrasonic time, and (D) for THF volume. Results were obtained for recovery of
249 fosetyl-aluminum. The design layout for the method using the CCD model is given in Table
250 S2.

251 The suitability of the CCD was determined by assessing various statistical parameters
252 such as the coefficients of determination (R^2), adjusted R^2 and predicted R^2 , the p-value, and
253 the lack-of-fit (LOF) test. The effect of the optimized parameters on the extraction of fosetyl-
254 aluminum was evaluated using ANOVA statistical analysis, and the results are presented in
255 Table 1. The high values of R^2 , adjusted R^2 , and predicted R^2 suggest that the proposed model
256 is well-suited to the experiment. The predicted R^2 value is in reasonable agreement with the
257 adjusted R^2 value, with a difference of 0.0077, which indicates that the CCD methodology is
258 being properly followed. The p-value, which should be less than 0.04 at the 95% confidence
259 level, is <0.0001 for this experiment, indicating that the parameters of the CCD have a
260 significant effect. The statistical analysis reveals that the proposed model is well-suited to the
261 experiment, as evidenced by the R^2 (0.9984), adjusted R^2 (0.9969), and predicted R^2 (0.9910)
262 values which are close to 1. The p-values for the model terms indicate that A, B, C, D, AB,
263 AD, BC, BD, CD, A^2 , B^2 , C^2 , and D^2 are all significant. Lack of Fit for the proposed method
264 is not significant. The final equation in terms of coded factors

$$\begin{aligned} 265 \text{ Recovery (\%)} = & +73.49 + 0.2722A - 5.74B + 1.54C + 5.88D - 3.16AB - 1.67AC - 4.47AD \\ 266 & + 3.14BC - 1.34BD + 2.77CD - 4.28A^2 - 7.23B^2 + 8.32C^2 + 7.02D^2 \end{aligned}$$

267 Furthermore, the effect of the signal-to-noise ratio on the CCD was evaluated using
268 adequate precision. To achieve statistical significance, the adequate precision must exceed 4.
269 According to the results presented in Table 1, the obtained adequate precision (105.91) was
270 significantly greater than the critical value. Figure 1 shows the actual vs predicted values
271 graph.



272 3D surface plots were used to plot the effect of binary interactions of optimized factors
273 on the recovery of fosetyl-aluminum. The effect of the IL volume versus pH on the recovery
274 of fosetyl-aluminum was given in Figure 2a. It can be seen that acceptable recoveries were
275 achieved, especially when the pH was less than 6. Interestingly, phase separation could not be
276 achieved due to decreased activity of IL binding sites in the basic region. The effect of
277 ultrasonic time versus IL volume on the recovery of fosetyl-aluminum was presented in
278 Figure 2b. To some extent, the recovery of fosetyl-aluminum was quantitative when
279 ultrasonic time and IL volumes were in the range of 8-10 min and 300-500 μL , respectively.
280 In particular, the recovery of fosetyl-aluminum was not quantitative at high ionic liquid
281 volumes. This may be attributed to insufficient sonication to achieve distribution in the
282 sample solution with increasing IL volume. The effect of THF volume versus IL volume on
283 the recovery of fosetyl-aluminum was shown in Figure 2c. THF (as a dispersive solvent)
284 helped to increase its interaction with fosetyl-aluminum by effectively dispersing IL in the
285 sample solution. In this way, the fosetyl-aluminum in the sample solution was easily
286 transferred to the IL phase. Due to this phenomenon, quantitative recoveries were obtained
287 when THF volume and IL volume were in the range of 380-490 μL and 330-450 μL ,
288 respectively.

289 In the optimization step, CCD was applied to maximize the recovery of fosetyl-
290 aluminum. According to the CCD, the maximum recovery was obtained using IL volume (410
291 μL), pH (5.2), ultrasonic time (2.5 min), and THF volume (480 μL). After five replicates, the
292 experimental recovery of fosetyl-aluminum was as high as 93.9%, which agrees with the
293 predicted recovery (93.4%) of the CCD with a 0.945 of desirability function (see Figure 3).
294 Therefore, these extraction conditions were selected as optimum values for the other studies
295 such as validation and analysis.

296 **3.2 Analytical parameter of the IL-UA-DLLME procedure**



297 Basic analytical parameters of the IL-UA-DLLME procedure were estimated using
298 optimized extracting conditions (IL volume 410 μL , pH 5.2, ultrasonic time 2.5, and THF
299 volume 480 μL). The linearity of the method was observed within the concentration range of
300 5-600 ng mL^{-1} with a high coefficient of determination (R^2) of 0.9914. The limit of detection
301 (LOD) and limit of quantification (LOQ) were calculated to be 1.5 ng mL^{-1} and 5.0 ng mL^{-1} ,
302 respectively. The percentage recovery for actual samples was between 94.2-98.6%, with an
303 EF of 114. The RSD was between 1.9-3.3%. The analytical performance of the IL-UA-
304 DLLME procedure is shown in the Table 2. The robustness of the method was tested for 10%
305 changes in basic analytical parameters (IL volume, pH, ultrasonic time, THF volume), and an
306 effective recovery ($\geq 93.8\%$) was obtained.

307 **3.3. Selectivity of the IL-UA-DLLME procedure-matrix species**

308 The matrix effect is an essential consideration in developing a new analytical method
309 and understanding its impact on the method can help in optimizing the method to provide
310 accurate and reliable results. In a new analytical method, it is crucial to assess the matrix
311 effect to ensure that the method can accurately measure the analytes of interest in the sample
312 matrix. In this method, the matrix effect of the most commonly existing 19 different types of
313 cations, anions, and organic compounds were studied. The tolerance limit was calculated as
314 “matrix species amount (ng mL^{-1})/ fosetyl-aluminum amount (ng mL^{-1}). A tolerance limit test
315 is required for an analytical method to determine the method's ability to measure a specific
316 analyte accurately and precisely within a predefined range. The tolerance limit test helps in
317 assessing the method's ability to meet the acceptance criteria and the regulatory requirements
318 for the specific application. Tolerance limit for the selected ions Na^+ (20000 ng mL^{-1}), Ca^{2+}
319 (20000 ng mL^{-1}), SO_4^{2-} (20000 ng mL^{-1}), CO_3^{2-} (15000 ng mL^{-1}), F^- (15000 ng mL^{-1}), $\text{C}_2\text{O}_4^{2-}$
320 (10000 ng mL^{-1}), Mg^{2+} (10000 ng mL^{-1}), Fe^{2+} (10000 ng mL^{-1}), Cd^{2+} (4000 ng mL^{-1}), and
321 Pb^{2+} (1000 ng mL^{-1}) was quite high. In case of ions presence, the recovery was 96-99% with



322 RSD 1.7-2.6%. For other organic species like boscalid (1000 ng mL⁻¹), metconazole (500 ng
323 mL⁻¹), tebuconazole (200 ng mL⁻¹), spiroxamine (200 ng mL⁻¹), cycloheximide (100 ng mL⁻¹),
324 chlorothalonil (100 ng mL⁻¹), carbendazim (100 ng mL⁻¹), azoxystrobin (50 ng mL⁻¹), and
325 triadimefon (50 ng mL⁻¹) the recovery was 94-97% with RSD 1.9-2.2%. This study reveals
326 that this method is highly selective and no considerable interference was observed. The
327 summary of this study is given in Table S3.

328 **3.4. Precision and robustness of IL-UA-DLLME procedure**

329 Precision in the context of analytical methods refers to the degree of agreement or
330 reproducibility between repeated measurements of the same sample under identical
331 experimental conditions. In other words, precision is a measure of how closely individual
332 measurements of a sample agree with each other. Inter-day and intra-day experiments were
333 performed for the estimation of the precision and accuracy of the assay. Three concentrations
334 of fosetyl-aluminum (10, 300, and 500 ng mL⁻¹) were tested for precision of the method (see
335 Table S4). The recover for intra-day (N=5) experiments was 94.8-97.8% with 2.5-3.8% of
336 RSD. For inter-day precision, a total of 15 experiments were performed on three consecutive
337 days (n=3x5). The recovery for inter-day experiments was 93.8-96.1% with 3.8-4.7% of RSD.

338 The robustness of an analytical method refers to the ability of the method to remain
339 unaffected by small variations in experimental conditions, such as changes in temperature,
340 pH, or sample preparation. An analytical method can produce consistent and reliable results
341 even when small changes in experimental conditions are introduced. Robustness is typically
342 evaluated by deliberately varying the experimental conditions within a certain range and
343 observing the effect on the analytical results. The degree of variation that the method can
344 tolerate while still producing reliable results is called the method's robustness (Ferreira et al.,
345 2017). Robustness was estimated for IL volume±10%, pH±10%, ultrasonic time±10% and
346 THF volume±10% (see Table S5). The volume of IL was in the range of 400-450 µL. pH was



347 changed in a range of 4.7-5.7. Ultrasonic time was varied in a range of 2.25-2.75 min. THF
348 volume was varied in the range of 430-530 μL . Results reveal that minor changes in
349 extraction conditions does not significantly affect the recovery of the IL-UA-DLLME
350 procedure for fosetyl-aluminum. It was concluded that the IL-UA-DLLME procedure is
351 robust for mild change (10%) in extraction parameters.

352 **3.5. Application of IL-UA-DLLME method for food and vegetable samples**

353 To validate the developed method, the IL-UA-DLLME procedure was used for the
354 analysis of fosetyl-aluminum in fruit and vegetable samples. Melon, watermelon, collards,
355 gherkin, cauliflower, radish, and zucchini were used as test plants. Fruits and vegetables were
356 obtained from plants grown under controlled conditions in a greenhouse. All samples were
357 spiked with concentrations of 100 ng mL^{-1} and 300 ng mL^{-1} of fosetyl-aluminum. The IL-
358 UA-DLLME procedure was then applied to these samples under optimized conditions. Five
359 replicate samples were used for analysis to get reliable results. For the reliability of the results
360 obtained, the same samples were also analyzed by independent method (Tóth et al., 2022).
361 Comprehensive results are given in Table 3. Recovery of fosetyl-aluminum was determined in
362 zucchini (94.7-96.2%), radish (97.1-98.6%), cauliflower (92.5-95.0%), gherkin (93.8-96.4%),
363 collards (95.5-97.6), watermelon (91.7-95.9), and melon (96.3-98.8%). Results reveal that the
364 IL-UA-DLLME procedure is applicable for fruit and vegetable samples.

365 **3.6. Comparison with previous studies**

366 In this study, important parameters (analytical methods, LOD, linearity range, %RSD, and
367 matrix) of this method were compared with recently reported methods in the literature. The
368 summary of this study is presented in Table 4. Only a few methods have been reported for
369 fosetyl-aluminum analysis in food samples. Lopez-Ruiz et al 2020. developed a method for
370 the analysis of fosetyl-aluminum in human blood serum by liquid chromatography-triple
371 quadrupole mass spectrometer. However, this method required complicated instrumentation,



372 and the overall procedure is more complex. Furthermore, this method required more time (40
373 minutes) for sample preparation (López-Ruiz et al., 2020). Raski et al. developed a method
374 based on ion chromatography for the analysis of fosetyl-aluminium in fruits and vegetables
375 (Rajski et al., 2018). The method is simple and robust however less sensitive, applicable only
376 at ppm level. RSD value is high (17%) and applicable within a limited range of concentration
377 (0.01-0.1 mg L⁻¹). Buiarelli et al. has described a different analytical approach for the
378 detection of fosetyl-aluminum in airborne particulate matter, which involves hydrophilic
379 interaction liquid chromatography coupled with tandem mass spectrometry. This method
380 required more time (60 minutes time) for sample preparation. This method required advanced
381 instrumentation (Buiarelli et al., 2018). Chamkasem et al. introduced a liquid
382 chromatography/tandem mass spectrometry approach for quantifying the presence of fosetyl-
383 aluminum in grapes. This method required advanced instrumentation and a complicated
384 sample preparation procedure. Furthermore, LOD for this method is quite higher than this
385 new method (Chamkasem, 2017). Li et al. established an analytical method using a procedure
386 of extraction coupled with hydrophilic interaction liquid chromatography-tandem mass
387 spectrometry to detect fosetyl-aluminum in wheat flour (Li et al., 2021). The method is
388 applicable for a wide range of concentrations (10–2000 µg Kg⁻¹) with a preconcentration
389 factor of 114. However, it involved complicated and advanced instrumentation and required
390 more time for sample preparation. Sadiq and Hammood have documented a procedure that
391 employs continuous flow injection and indirect photometric detection for detecting fosetyl-
392 aluminum in commercial formulations. However, this method applies to only commercial
393 formulations and may not apply to complex matrices. Secondly, the method is more time-
394 consuming and required advanced instrumentation (Sadiq and Hammood, 2022).

395 The results of this study show that the IL-UA-DLLME procedure is the most sensitive
396 method among available approaches for same type of samples. It involves simple



397 instrumentation like a UV-Visible spectrophotometer and an easy extraction procedure. There
398 are no complicated steps and the least time is required for the extraction procedure.
399 Furthermore, this method uses IL which is considered as a green solvent system. The method
400 has been applied to multiple fruit and vegetable samples and was found highly selective.
401 Furthermore, for sample preparation, plants and vegetables were grown under controlled
402 conditions in a greenhouse which is another addition to the sample preparation process. Based
403 on the results obtained it was evidently proved that this method can be effectively used for
404 fosetyl-aluminum in food samples.

405 **4. Conclusions**

406 In conclusion, the proposed method using IL-based UA-DLLME coupled with
407 chemometric modeling was successfully applied for the analysis of fosetyl-aluminum in
408 various fruit and vegetable samples. The use of this method demonstrated several advantages,
409 including high selectivity and sensitivity, short analysis time, and low consumption of organic
410 solvents. The results obtained for the optimized experimental conditions were in good
411 agreement with the expected values, indicating good accuracy and reliability of the proposed
412 model. The IL-UA-DLLME method was characterized by wide linearity (5-600 ng mL⁻¹), low
413 limit of detection (1.5 ng mL⁻¹) and limit of quantification (5.0 ng mL⁻¹), enrichment factor of
414 114, very good precision (RSD in the range of 1.9-3.3%) as well as robustness. Stable and
415 effective extraction conditions were developed, ensuring high and repeatable recovery values
416 (94.2-98.6%). Therefore, the IL-UA-DLLME method can be considered as a reliable and
417 efficient alternative method for the determination of fosetyl-aluminum in fruit and vegetable
418 samples possible to be applied in routine analysis.

419 **Compliance with Ethical Standards**

420 None.

421 **Informed Consent**



422 Not applicable.

423 References

424

425

426

427

428

429

430 Authority, E. F. S., Arena, M., Auteri, D., Barmaz, S., Brancato, A., Brocca, D., Villamar-
431 Bouza, L. 2018. Peer review of the pesticide risk assessment of the active substance spinosad. *EFSA*
432 *Journal*, 16(5).

433 Bahram, M., Shokri, L., Mohseni, N. 2016., Application of Central Composite Design for
434 Optimization of Coacervative Extraction of Cu (II) Using Anionic Surfactant. *Analytical and*
435 *Bioanalytical Chemistry Research*, 3(1), 19-27.

436 Bohinc, T., VUČAJNK, F., Trdan, S., 2019. The efficacy of environmentally acceptable
437 products for the control of major potato pests and diseases. *Zemdirbyste-Agriculture*, 106(2).

438 Buiarelli, F., Di Filippo, P., Riccardi, C., Pomata, D., Marsiglia, R., Console, C., Puri, D.,
439 2018. Hydrophilic interaction liquid chromatography-tandem mass spectrometry analysis of fosetyl-
440 aluminum in airborne particulate matter. *Journal of Analytical Methods in Chemistry*, 2018.

441 Chamkasem, N. 2017. Determination of glyphosate, maleic hydrazide, fosetyl aluminum, and
442 ethephon in grapes by liquid chromatography/tandem mass spectrometry. *Journal of agricultural and*
443 *food chemistry*, 65(34), 7535-7541.

444 Chen, G., Jamro, I. A., Samo, S. R., Wenga, T., Baloch, H. A., Yan, B., Ma, W. 2020.
445 Hydrogen-rich syngas production from municipal solid waste gasification through the application of
446 central composite design: an optimization study. *International Journal of Hydrogen Energy*, 45(58),
447 33260-33273.

448 Chiappe, C., Mezzetta, A., Pomelli, C. S., Iaquaniello, G., Gentile, A., Masciocchi, B. 2016.
449 Development of cost-effective biodiesel from microalgae using protic ionic liquids. *Green*
450 *Chemistry*, 18(18), 4982-4989.

451 Farajzadeh, M. A., Mohebbi, A., Pazhohan, A., Nemati, M., Mogaddam, M. R. A. 2020. Air-
452 assisted liquid-liquid microextraction; principles and applications with analytical instruments. *TrAC*
453 *Trends in Analytical Chemistry*, 122, 115734.

454 Ferreira, S. L., Caires, A. O., Borges, T. D. S., Lima, A. M., Silva, L. O., dos Santos, W. N.
455 2017. Robustness evaluation in analytical methods optimized using experimental
456 designs. *Microchemical Journal*, 131, 163-169.

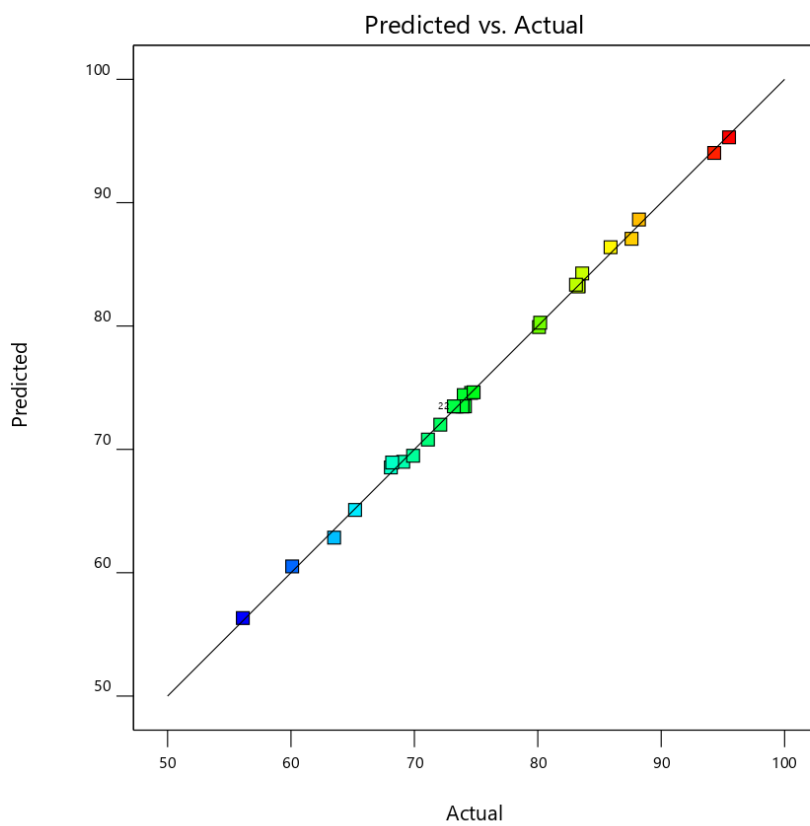
457 Gormez, E., Golge, O., González-Curbelo, M. Á., Kabak, B. 2022. Monitoring and exposure
458 assessment of fosetyl aluminium and other highly polar pesticide residues in sweet
459 cherry. *Molecules*, 28(1), 252.

- 460 Han, D., Tang, B., Ri Lee, Y., Ho Row, K., 2012. Application of ionic liquid in liquid phase
461 microextraction technology. *Journal of separation science*, 35(21), 2949-2961.
- 462 Haq, H. U., Balal, M., Castro-Muñoz, R., Hussain, Z., Safi, F., Ullah, S., Boczkaj, G. 2021.
463 Deep eutectic solvents based assay for extraction and determination of zinc in fish and eel samples
464 using FAAS. *Journal of Molecular Liquids*, 333, 115930.
- 465 Haq, H. U., Wali, A., Safi, F., Arain, M. B., Kong, L., Boczkaj, G. 2023. Natural deep eutectic
466 solvent based ultrasound assisted liquid-liquid micro-extraction method for methyl violet dye
467 determination in contaminated river water. *Water Resources and Industry*, 29, 100210.
- 468 Huddleston, J. G., Visser, A. E., Reichert, W. M., Willauer, H. D., Broker, G. A., Rogers, R.
469 D., 2001. Characterization and comparison of hydrophilic and hydrophobic room temperature ionic
470 liquids incorporating the imidazolium cation. *Green chemistry*, 3(4), 156-164.
- 471 Kiselev, E. G., Prudnikova, S. V., Streltsova, N. V., Volova, T. G., 2022. Effectiveness of
472 slow-release fungicide formulations for suppressing potato pathogens. *Pest Management
473 Science*, 78(12), 5444-5455.
- 474 Li, X., Wang, S., Guo, Z., Li, X., Zhang, Q., Li, H., 2021. Determination of fosetyl-aluminum
475 in wheat flour with extract-dilute-shoot procedure and hydrophilic interaction liquid chromatography
476 tandem mass spectrometry. *Separations*, 8(11), 197.
- 477 Llaver, M., Oviedo, M. N., Fiorentini, E. F., Quintas, P. Y., Wuilloud, R. G., 2021. Analytical
478 developments and applications of ionic liquids for environmental studies. *Trends in Environmental
479 Analytical Chemistry*, 31, e00131.
- 480 López-Ruiz, R., Romero-González, R., Frenich, A. G., 2020. Simultaneous determination of
481 polar pesticides in human blood serum by liquid chromatography coupled to triple quadrupole mass
482 spectrometer. *Journal of Pharmaceutical and Biomedical Analysis*, 190, 113492.
- 483 Makoś, P., Przyjazny, A., Boczkaj, G. 2018. Hydrophobic deep eutectic solvents as “green”
484 extraction media for polycyclic aromatic hydrocarbons in aqueous samples. *Journal of
485 Chromatography A*, 1570, 28-37.
- 486 Ngan, C. L., Basri, M., Lye, F. F., Masoumi, H. R. F., Tripathy, M., Karjiban, R. A., Abdul-
487 Malek, E., 2014. Comparison of Box–Behnken and central composite designs in optimization of
488 fullerene loaded palm-based nano-emulsions for cosmeceutical application. *Industrial Crops and
489 Products*, 59, 309-317.
- 490 Pérez-Lucas, G., Vela, N., El Aatik, A., Navarro, S. 2019. Environmental risk of groundwater
491 pollution by pesticide leaching through the soil profile. *Pesticides-use and misuse and their impact in
492 the environment*, 1-28.
- 493 Rajski, Ł., Díaz Galiano, F. J., Cutillas, V., Fernández-Alba, A. R., 2018. Coupling ion
494 chromatography to Q-orbitrap for the fast and robust analysis of anionic pesticides in fruits and
495 vegetables. *Journal of AOAC International*, 101(2), 352-359.
- 496 Rasheed, S., Hashmi, I., Zhou, Q., Kim, J. K., Campos, L.C., 2023. Central composite
497 rotatable design for optimization of trihalomethane extraction and detection through gas
498 chromatography: a case study. *International Journal of Environmental Science and Technology*, 20(2),
499 1185-1198.
- 500 Rouabhi, R. 2010. Introduction and Toxicology of Fungicides, Fungicides, Odile Carisse
501 (Ed.), ISBN: 978-953-307-266-1. *InTech*, Available from: <http://www.intechopen.com/books/fungicides/introduction-and-toxicology-of-fungicides>, 364-382.



- 503 Rykowska, I., Ziemblińska, J., Nowak, I., 2018. Modern approaches in dispersive liquid-liquid
504 microextraction (DLLME) based on ionic liquids: A review. *Journal of molecular liquids*, 259, 319-
505 339.
- 506 Rutkowska, E., Łozowicka, B., Kaczyński, P., 2018. Modification of multiresidue QuEChERS
507 protocol to minimize matrix effect and improve recoveries for determination of pesticide residues in
508 dried herbs followed by GC-MS/MS. *Food Analytical Methods*, 11(3), 709-724.
- 509 Sadiq, H. A., Hammood, M. K., 2022. A Continuous Flow Injection/Indirect Photometric
510 Method for the Detection of Fosetyl Aluminum in Commercial Pesticide
511 Formulations. *ChemistrySelect*, 7(15), e202104605.
- 512 Shahid, M., Khan, M. S., Syed, A., Marraiki, N., Elgorban, A. M., 2021. Mesorhizobium
513 ciceri as biological tool for improving physiological, biochemical and antioxidant state of Cicer
514 aritenum (L.) under fungicide stress. *Scientific Reports*, 11(1), 9655.
- 515 Shahid, M., Khan, M. S., Zaidi, A. 2020. Fungicide toxicity to legumes and its microbial
516 remediation: A current perspective. *Pesticides in Crop Production: Physiological and Biochemical
517 Action*, 15-33.
- 518 Sharma, A., Kumar, V., Shahzad, B., Tanveer, M., Sidhu, G. P. S., Handa, N., Thukral, A. K.,
519 2019. Worldwide pesticide usage and its impacts on ecosystem. *SN Applied Sciences*, 1, 1-16.
- 520 Tóth, E., Tölgyesi, Á., Bálint, M., Ma, X., Sharma, V. K. 2022. Separation of fosetyl and
521 phosphonic acid in food matrices with mixed-mode HPLC column coupled with tandem mass
522 spectrometric detection and method application to other highly polar pesticides. *Journal of
523 Chromatography B*, 1189, 123083.
- 524 Tudi, M., Daniel Ruan, H., Wang, L., Lyu, J., Sadler, R., Connell, D., Chu, C., Phung, D.T.,
525 2021. Agriculture development, pesticide application and its impact on the environment. *Int. J.
526 Environ. Res. Public Health* 18.
- 527 Tudi, M., Daniel Ruan, H., Wang, L., Lyu, J., Sadler, R., Connell, D., Phung, D. T. 2021.
528 Agriculture development, pesticide application and its impact on the environment. *International
529 journal of environmental research and public health*, 18(3), 1112.
- 530 Ullah, S., Haq, H. U., Salman, M., Jan, F., Safi, F., Arain, M. B., Boczkaj, G., 2022.
531 Ultrasound-Assisted Dispersive Liquid-Liquid Microextraction Using Deep Eutectic Solvents (DESs)
532 for Neutral Red Dye Spectrophotometric Determination. *Molecules*, 27(18), 6112.
- 533 Van de Wouw, A. P., Scanlan, J. L., Marcroft, S. J., Smith, A. J., Sheedy, E. M., Perndt, N.
534 W., Huyghe, C., 2021. Fungicide sensitivity and resistance in the blackleg fungus, *Leptosphaeria
535 maculans*, across canola growing regions in Australia. *Crop and Pasture Science*, 72(12), 994-1007.
- 536 Zubrod, J. P., Bundschuh, M., Arts, G., Brühl, C. A., Imfeld, G., Knäbel, A., Schäfer, R. B.,
537 2019. Fungicides: an overlooked pesticide class?. *Environmental science & technology*, 53(7), 3347-
538 3365.
- 539





540

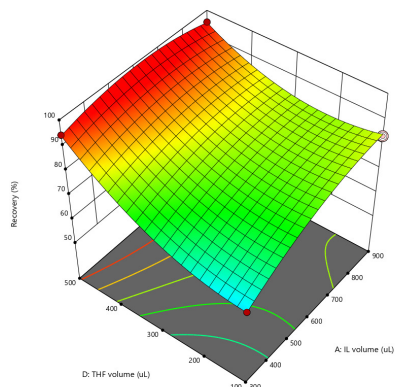
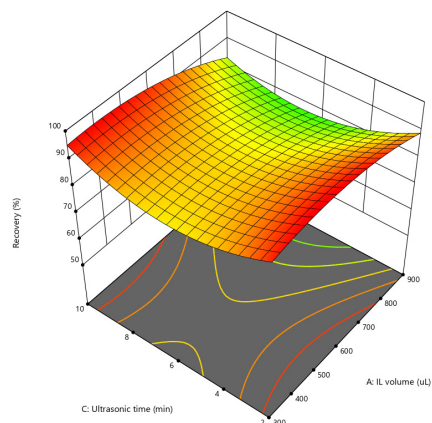
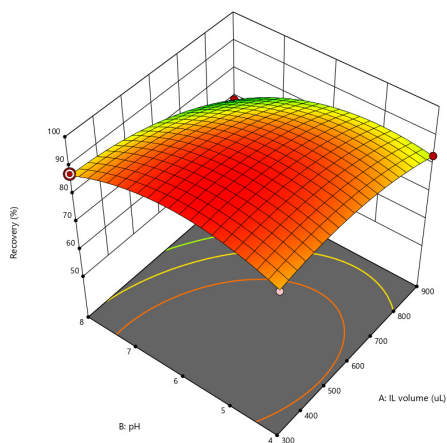
541

Figure 1. Agreement between experimental data and CCD's prediction data

542

543

544



545

(a)

(b)

546

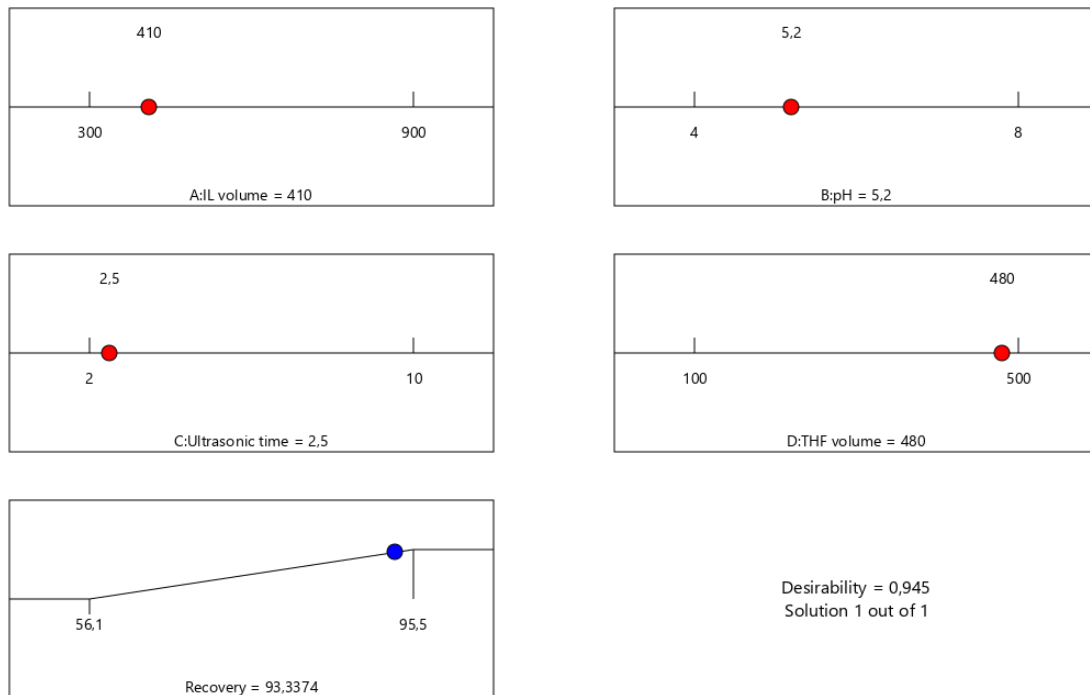
(c)

547 Figure 2 (a-c). 3D surface response plot for optimized variables, (a) IL volume and pH; (b) IL volume
 548 and ultrasonic time; (c) IL volume and THF volume

549

550

551



552

553

554

Figure 3. The optimum values predicted by the model for the variables

555

556

557 Table 1. ANOVA for quadratic model

558

Source	Sum of Squares	Mean Square	F-value	p-value	
Model	2550,60	182,19	672,76	< 0.0001	significant
A	1.33	1.33	4.93	0.0423	
B	593.98	593.98	2193.38	< 0.0001	
C	42.63	42.63	157.41	< 0.0001	
D	623.04	623.04	2300.72	< 0.0001	
AB	160.02	160.02	590.92	< 0.0001	
AC	44.89	44.89	165.77	< 0.0001	
AD	320.41	320.41	1183.18	< 0.0001	
BC	157.50	157.50	581.61	< 0.0001	
BD	28.62	28.62	105.69	< 0.0001	
CD	123.21	123.21	454.98	< 0.0001	
A ²	47.40	47.40	175.03	< 0.0001	
B ²	135.33	135.33	499.73	< 0.0001	
C ²	179.47	179.47	662.73	< 0.0001	
D ²	127.78	127.78	471.87	< 0.0001	
Lack of Fit	3.41	0.3407	2.60	0.1515	not significant
<i>Fit Statistics</i>					
R ²	0.9984		Predicted R ²	0.9910	
Adjusted R ²	0.9969		Adeq. Precision	105.9189	

559

560

561

562

563

564

565

566

567

568

569

570

571



572 Table 2. Analytical performance of the IL-UA-DLLME procedure

Parameters	Value
Working range, ng mL ⁻¹	5-600
Coefficient of determination (R ²)	0.9914
LOD, ng mL ⁻¹	1.5
LOQ, ng mL ⁻¹	5.0
EF	114
*Recovery%	94.2-98.6
*RSD%	1.9-3.3

573 * At concentrations of 10, 300 and 500 ng mL⁻¹ of fosetyl-aluminum (n=3).

574 LOD: Limit of detection

575 LOQ: Limit of quantification

576 EF: Enhancement factor

577

578

579

580

581

582

583

584

585

586

587

588

589

590

591

592

593

594

595

596

597

598

599

600



601 Table 3. Application results of the IL-UA-DLLME method to fruit and vegetable samples (n=5)

Samples	Spiked (ng mL ⁻¹)	Found (ng mL ⁻¹)	Matrix effect (%)	Recovery (%)	Found by independent method (ng mL ⁻¹)
Zucchini	-	25±1	4.8	-	24±2
	100	120±7		95±2	122±4
	300	314±15		96±3	311±12
Radish	-	32±3	6.3	-	34±2
	100	129±7		97±1	133±4
	300	328±20		96±2	325±13
Cauliflower	-	17±2	5.9	-	14±1
	100	110±6		93±4	112±4
	300	302±11		95±2	299±15
Gherkin	-	25±2	8.7	-	27±3
	100	119±7		94±3	123±6
	300	314±19		96±3	311±21
Collards	-	13±1	3.1	-	14±1
	100	108±4		95±4	105±3
	300	306±14		98±1	301±12
Watermelon	-	62±4	6.8	-	68±3
	100	153±8		91±5	151±7
	300	350±18		96±3	358±14
Melon	-	29±3	9.1	-	24±2
	100	126±7		97±2	130±6
	300	326±20		99±2	331±18

602 * Mean ± standard deviation.

603

604 Table 4. Comparison of the method with other approaches.

Analytical method	Extraction solvents	LOD	Linearity range	RSD (%)	Enrichment factor	Samples	References
¹ LC-TQMS	Water, acetonitriles and n-hexane	0.01 mg L ⁻¹	0.01-0.1 mg L ⁻¹	17	----	human blood serum	(López-Ruiz et al., 2020)
² IC-QOMA	Methanol and water	0.01 mg Kg ⁻¹	0.01–0.50 mg Kg ⁻¹	----	40	Fruits and Vegetables	(Rajski et al., 2018)
³ MS-NEI	ASE Dionex and water	0.3 ng mL ⁻¹	1-700 ng mL ⁻¹	10	75	Particulate Matter	(Buiarelli et al., 2018)
⁴ LC-TMS;	HOAc, Na ₂ EDTA, MeOH/H ₂ O	29 µg Kg ⁻¹	10-1000 µg Kg ⁻¹	17	----	Grapes	(Chamkasem, 2017)
⁵ HI-LC-TMS	Water and acetonitrile	5 µg Kg ⁻¹	10–2000 µg Kg ⁻¹	6.2	114	Wheat	(Li et al., 2021)
⁷ CFI-IP	Methanol, acetonitrile	0.0041 mmol L ⁻¹	0.005–1.8 mmol L ⁻¹	2.1	--	Commercial formula	(Sadiq and Hammood, 2022)
⁸ IL-UA-DLLE	⁹ IL	1.5 µg L ⁻¹	5-600 µg L ⁻¹	1.9-3.3	114	Fruits, vegetables	Present method

605 ¹LC-TQMS; Liquid chromatography coupled to triple quadrupole mass spectrometer, ²IC-QOMA; Ion chromatography coupled to a quadrupole Orbitrap mass analyzer, ³MS-
606 NEI; mass spectrometry-negative electrospray ionization, ⁴LC-TMS; Liquid Chromatography/Tandem Mass Spectrometry, ⁵HI-LC-TMS; Hydrophilic interaction
607 chromatography tandem mass spectrometry, ⁶IC-TMS; Ion Chromatography–Tandem Mass Spectrometry, ⁷CFI-IP; Continuous Flow Injection/Indirect Photometry, ⁸IL-UA-
608 DLLE; Ionic liquid based ultrasonic-assisted dispersive liquid-liquid micro-extraction, ⁹IL; Ionic liquid (1-ethyl-3-methylimidazolium hydrogen sulfate).

